Variable length LMS adaptive filter for carrier phase multipath mitigation

Huicui Liu [1, 2], Cemal Ozer Yigit[2], Shaocheng Zhang[2], Chris Rizos[2]
1. School of Electronic Science and Engineering, National Univ. of Defense Technology, Changsha 410073, China
2. School of Surveying and Spatial Information Systems, University of New South Wales, Sydney, 2052, Australia

Abstract

Multipath effects on carrier phase measurements are the major error source for short baseline positioning scenarios. One type of data processing techniques that can be used to mitigate multipath effects, Least Mean Square (LMS) filters, is investigated in this paper.

The strong correlation between two successive days' multipath effects on carrier phases double-differenced (DD) data, due to the fact that the antennas are static and the surrounding environment is unchanged, is investigated. Based on this fact, the multipath effects can be extracted and removed by a LMS filter in order to achieve higher positioning accuracy. In this paper the performance of two LMS adaptive filters, the standard LMS adaptive filter and the variable length LMS (VLLMS) adaptive filter, are studied. This paper reports the results from an analysis of observation data collected in a short baseline experiment.

Keywords: GPS, multipath, carrier phase, LMS, adaptive filter.

Introduction

The multipath error in GPS carrier phase measurements is negligible compared to the multipath error on pseudorange measurements. As long as the multipath-to-direct ratio is less than or equal to unity and the delay-lock-loop maintains track on the correlation function of the direct path, the magnitude of the carrier phase error due to a single multipath signal is less than or equal to a quarter of the wavelength as a consequence of the multipath signal being orthogonal to the direct signal (Kaplan and Hegarty, 2006). However, the multipath error is still a major error source in the case of precise positioning, after the atmospheric delay effects and satellite orbit error are accounted for.

Multipath mitigation technologies or algorithms can be divided into three categories: antenna design, signal processing (or receiver design), and data processing. The widely-used choke ring antenna (Fillippov, 1998; Tranquilla, 1994), for example, can mitigate multipath signals from horizontal directions. Many signal processing technologies such as MET (Townsend and Fenton, 1994) and MEDLL (Van Nee, 1994; Van Nee, 1992; Townsend, 2000) behave well when the multipath delay is more than 0.1chips. However, when the reflectors are higher than the antenna and the multipath delay is less than 0.1chips, data processing techniques are a better way to address the multipath problem. Many multipath mitigation data processing techniques have been developed by researchers. For instance, in Ge et al (2000) the Least Mean Square (LMS) adaptive filter was first applied for GPS multipath mitigation. However, this LMS filter had both fixed tap numbers and fixed step-size. In this paper an enhanced LMS filter with variable length, known as a VLLMS adaptive filter (Bilcu et al, 2002) is used to mitigate multipath effects in carrier phase observations.

Multipath effects in carrier phase double-differenced (DD) data

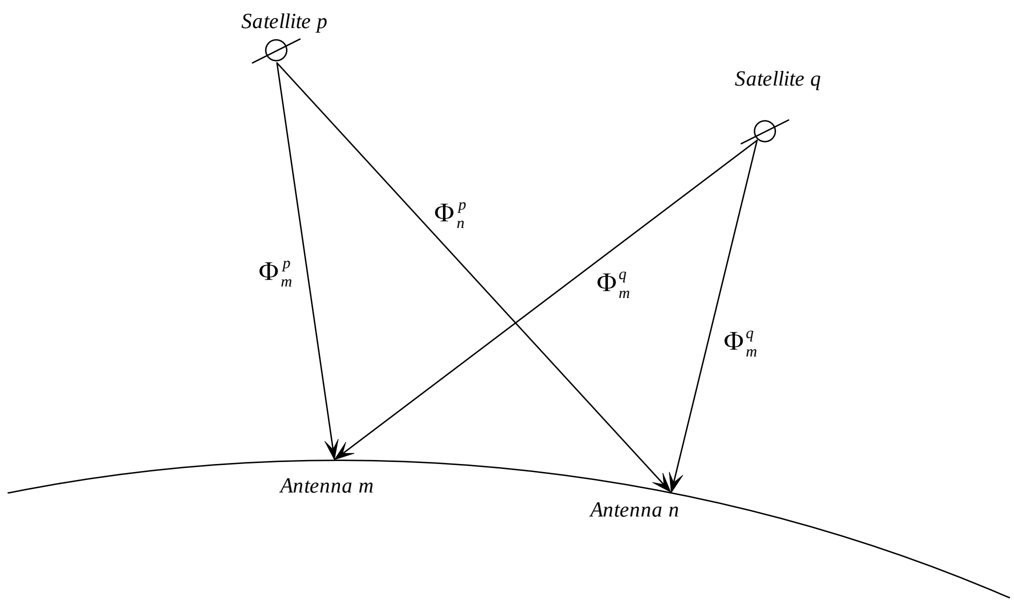

Figure 1: Double-differenced GPS data on a baseline and the geometric relations

Multipath effects on carrier phase can be calibrated using double-differenced (DD) data. Figure 1 shows the geometric relations of a single baseline. M and n represent two antennas, while p and q represent two satellites. The carrier phase observation data of satellite $i(i = p,q)$ received by antenna $j(j = m,n)$ can be written as (Kaplan and Hegarty, 2006):

$$\Phi_j^i = \phi_j^i - \phi^i + N_j^i + MP_j^i + f\tau_i + f\tau_j - \beta_j^i + \delta_j^i + \sigma_j^i \tag{1}$$

where:

ϕ_j^i is the receiver-measured satellite signal phase,

ϕ^i is the transmitted satellite signal phase,

N_j^i is the unknown integer number of carrier cycles,

MP_j^i is the phase error due to multipath effects,

τ_i and τ_j are the associated satellite and receiver clock bias respectively,

f is the carrier frequency,

β_j^i is the phase error due to ionospheric delay,

δ_j^i is the phase errors due to tropospheric delay, and

σ_j^i is the phase error due to other sources (including noise).

The carrier phase DD data associated with the two satellites and the two receiver antennas can be defined as:

$$DD = (\Phi_m^p - \Phi_m^q) - (\Phi_n^p - \Phi_n^q) = \Delta\phi + \Delta N + \Delta I + \Delta T + \Delta MP + \Delta\sigma \tag{2}$$

With the formation of the DD, the receiver and satellite clock-biases are cancelled (Kaplan and Hegarty, 2006). The remaining components are a phase term ($\Delta\phi$) representing the linear combination of carrier-phase measurements, the integer term (ΔN) consisting of the combined unknown integer ambiguities, multipath effects combination (ΔMP) and a system phase-noise term ($\Delta\sigma$) attributable primarily to receiver effects (Walsh, 1992). ΔI and ΔT are the combined ionospheric effects and tropospheric effects, respectively. In particular,

$$\Delta MP = (MP_m^p - MP_m^q) - (MP_n^p - MP_n^q) \tag{3}$$

In order to calibrate multipath effects, the baseline between the two antennas should be comparatively short (Kaplan and Hegarty, 2006), in order that the ionospheric and tropospheric effects can be assumed to cancel. Then the multipath effect is the dominant error component in the DD. That means a short baseline scenario is required. In the short baseline scenario, the multipath effects on carrier phase measurements made to a certain satellite by a specific antenna can be studied if the followings conditions are satisfied:

(a) One antenna (the “base antenna”) should be located in an open multipath-free area while the other (the “rover antenna”) is assumed to be multipath-effected;
(b) During the observation period, a satellite with a high elevation is observable so that it could be considered as multipath-free, and serves as the “reference satellite”.
(c) The two antennae are both static;

With (a),(b)and equation (3), the multipath effects on DD data are equivalent to the multipath effects of the non-reference satellite of the rover receiver.

With (c), the multipath effect on carrier phase at some epoch is correlated with the multipath effect at the same epoch of the next sidereal day due to the fact that the azimuth and elevation of the GPS satellites and the receiver-reflectors’ locations repeat every sidereal day (approximately four minutes shorter than a mean solar day), Therefore multipath effects can be removed from carrier phase data by making use of the correlation characteristics. Subsequently, the positioning calculation based on the modified observation data can achieve higher accuracy.

The short-baseline experiment

A short baseline experiment was carried out to investigate the multipath effects on carrier phase double-differenced data. The experiment involved a baseline approximately 200m in length, lasted for two successive days, and was carried out in Centennial Park in Sydney (Australia) (Figure 2). The base antenna was in an open, multipath-free playground area in Centennial Park (Figure 4) while the rover antenna was located near the Federal Pavilion in Centennial Park (Figure 3). The experiments were carried out from about 10:00am to 12:00pm (GMT+10), 10th and 11th, September 2008, when satellite PRN 18 reached its peak elevation. Two sets of Leica GX1230 GNSS receivers were used in this experiment. The rover antenna type was the Leica AX1202 and the base antenna was the Leica AT504.

Figure 5 shows the elevations of five satellites visible during the experiments. There were also some others satellites in the sky at the same time but only these five were used for positioning.

Figure 2: The short baseline experiment environment (from Google Earth).

The carrier phase DD data associated with Rover and Base are shown in Figure 6, where the reference satellite is PRN18. In Figure 6, the first day's data is from 10:24:25 to 11:22:45 (GMT+10, sampled at 0.2Hz) while the second day's data is four minutes earlier. The correlation between the two days' L1 carrier phase DD data can be clearly seen and the correlated part is mainly due to multipath effects. In addition, the multipath effects on the first 300 samples of the first plot, and the multipath effects on the last 400 samples of the third plot, are worse than those for the same time period in the other three plots. The reason can be found in Figure 5, which shows that the elevations of satellites PRN6 and PRN16 are the lowest of the five satellites observed.

Figure 3: Rover receiver in Centennial Park, Sydney.

Figure 4: Base receiver in Centennial Park, Sydney.

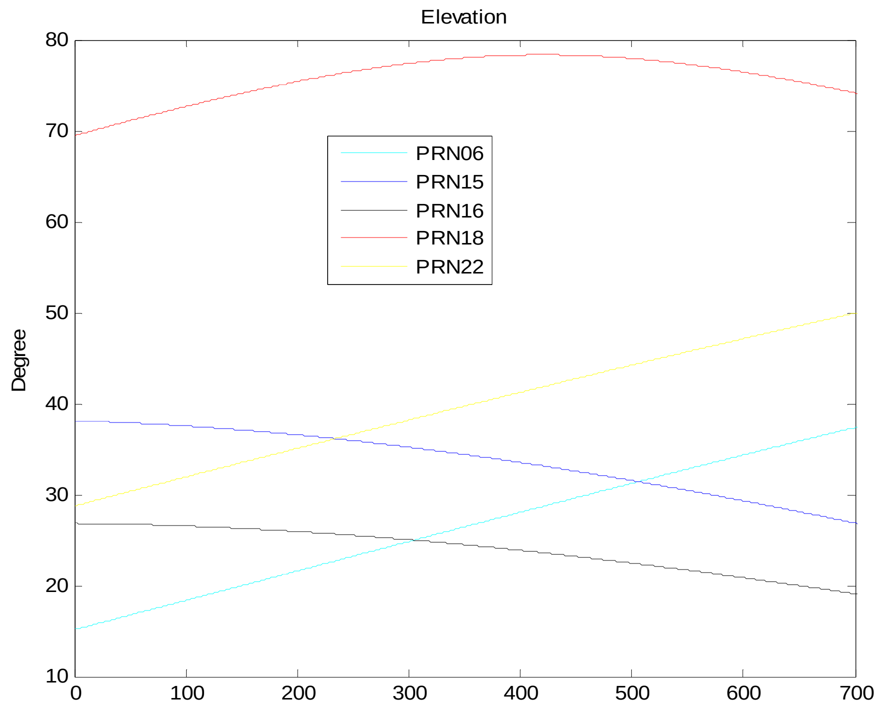

Figure 5: Elevation angles of the satellites during the experiments.

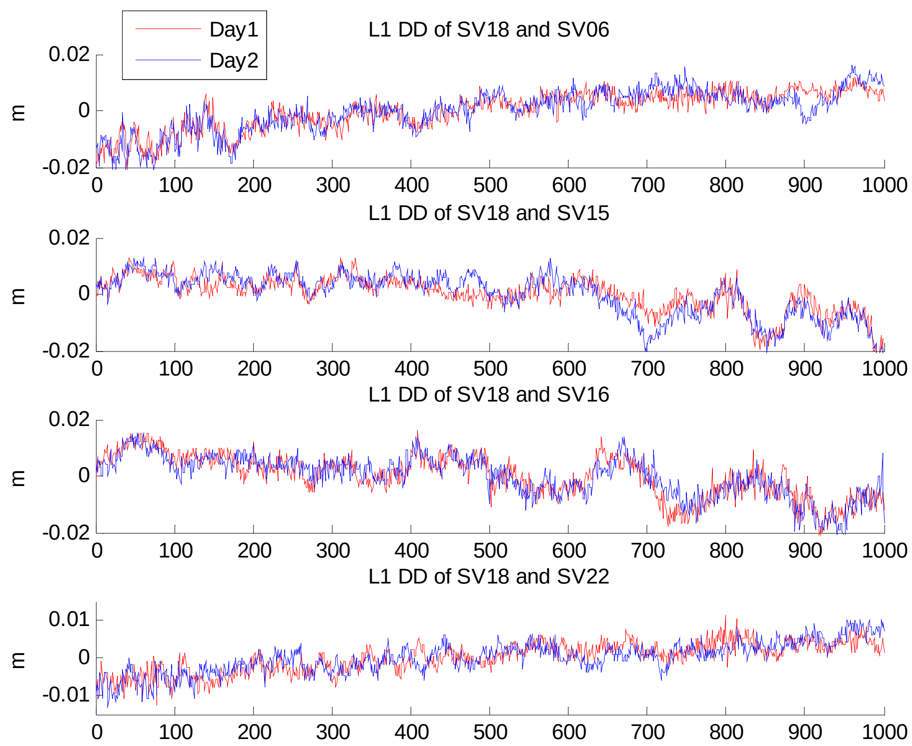

Figure 6: L1 Carrier phase DD data involving Rover and Base receivers.

The LMS adaptive filter

Multipath mitigation using an LMS adaptive filter was first proposed by Ge (1999). The general configuration of the LMS adaptive filter is shown in Figure 7. The input signal can be represented as:

$$r(n) = x(n) + u(n) \tag{4}$$

where $x(n)$ is the desired signal and $u(n)$ is the noise distortion. The three signals have the same vector length N . Assume $d(n)$ is the reference signal.

In order to extract the desired signal from the input signal, $x(n)$, $u(n)$ and $d(n)$ should fulfill the following conditions (Ge et al, 2000):

$$\begin{aligned} &E[d(n)x(n-k)] = p(k); n,k = 1,...N \\ &E[x(n)u(n-k)] = 0; n,k = 1,...N \\ &E[d(n)u(n-k)] = 0; n,k = 1,...N \end{aligned} \tag{5}$$

The multipath effects on pseudorange observations on a certain day can be written as Equation (4), where $x(n)$ is the multipath effect sequence and $u(n)$ is noise. The multipath effect sequence for another day is then expressed as:

$$d(n) = x'(n) + u'(n) \tag{6}$$

Where $x'(n)$ and $u'(n)$ have similar definitions as $x(n)$ and $u(n)$. The four vector lengths are N. $x(n)$, $x'(n)$, $u(n)$ and $u'(n)$ must satisfy equation(5):

$$\begin{aligned} &E[d(n)x(n-k)] = E[x(n)x(n-k)] = p(k); n,k = 1,...N \\ &E[x(n)u(n-k)] = 0; n,k = 1,...N \\ &E[d(n)u(n-k)] = E[u'(n)u(n-k)] = 0; n,k = 1,...N \end{aligned} \tag{7}$$

In this way the LMS filter can extract multipath effects from pseudorange observations.

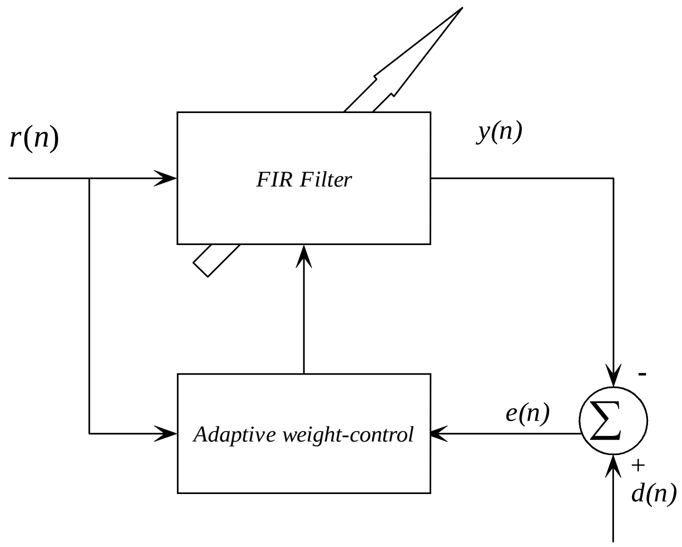

Figure 7: LMS filter configuration.

In Figure 7, $y(n)$ and $e(n)$ are the output of the filter and the estimation error respectively. The filter coefficients $w(n)$ with length M are controlled by an adaptive weight-control unit in which the least-mean-square algorithm has been introduced. $w(n)$ can be expressed as:

$$w_i(n) = w_{i-1}(n) + \mu e(n) r(n-1) \quad (8)$$

where μ is the step-size parameter; $i = 0,1...,M-1$ and $n = 0,1...,N-1$. So $y(n)$ and $e(n)$ can be expressed as:

$$y(n) = \sum_{i=0}^{M-1} w_i(n) r(n-i) \quad (9)$$

$$e(n) = d(n) - y(n). \quad (10)$$

The filter length M and the step-size parameter μ should be carefully chosen to make sure that the LMS algorithm converges rapidly and is stable. Haykin (2002) and Proakis (2001) discuss how to select the appropriate filter length and step-size parameter.

The variable length LMS adaptive filter (VLLMS adaptive filter)

The LMS filter can be applied very easily hence it has become very popular. However, almost all implementations known to the authors use some predefined values which do not change during the processing. Although there are some implementations of variable length LMS adaptive filters (see Pritzker and Feuer, 1991), their performance is not steady.

In Bilcu et al (2002), another variable LMS adaptive filter was introduced whose configuration is illustrated in Figure 8:

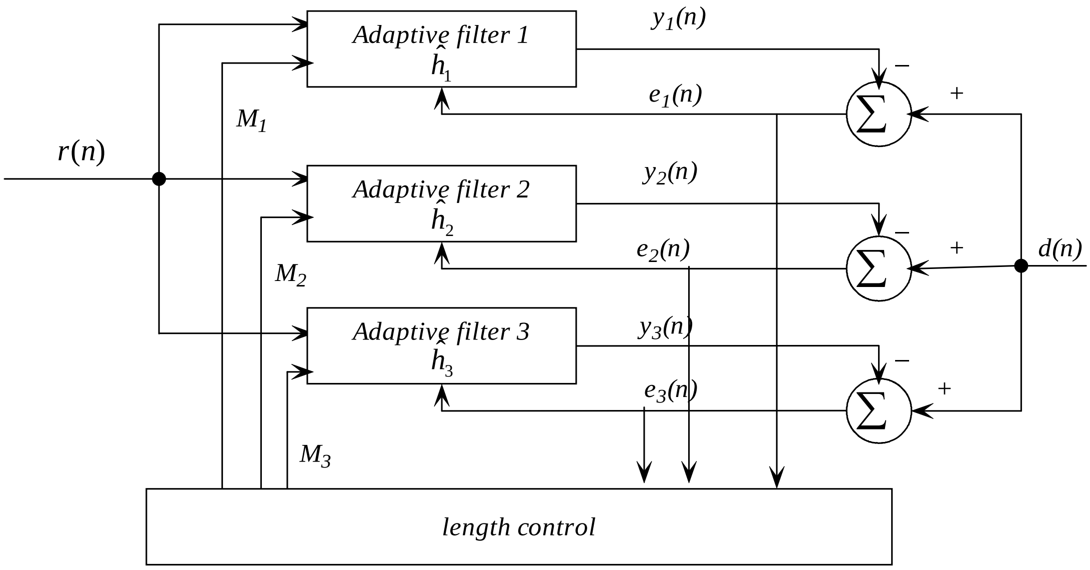

Figure 8: VLLMS filter configuration.

There are three parallel filters and each of them is the same as that in Figure 8. The length of these filters are M_1, M_2 and M_3. The three estimation errors $e_1(n)$, $e_2(n)$ and $e_3(n)$ are imported into a length control unit which computes some estimates of the Mean Square Error (MSE) for each filter and based on these estimates the updated filter lengths are generated. The algorithm can be summarised as follows:

1) Initialization:

$$M_1(0) = M_0, M_2(0) = M_0 + 1, M_3(0) = M_0 + 2$$
$$\hat{h}_1(0) = 0_{N_1}, \hat{h}_2(0) = 0_{N_2}, \hat{h}_3(0) = 0_{N_3} \quad (11)$$
$$\mu_1(0) = \frac{\mu M_0}{M_1(0)}, \mu_2(0) = \frac{\mu M_0}{M_2(0)}, \mu_2(0) = \frac{\mu M_0}{M_2(0)}$$

2) For each k=1,2,…:

a) Compute the output errors:

$$e_l(k) = d(k) - \sum_{i=1}^{M_1} \hat{h}_{li}(k) r(k-i+1), l = 1,2,3 \quad (12)$$

where $\hat{h}_{li}(k)$ is the i^{th} coefficient of the l^{th} adaptive filter.

b) Update the coefficients:

$$\hat{h}_l(k+1) = \hat{h}_l(k) + \mu_l(k) r_l(k) e_l(k), l = 1,2,3 \quad (13)$$

c) At each L^{th} iteration(where L is an integer parameter)do:

- Compute the following averages:

$$m_l = \frac{1}{L} \sum_{j=k-L+1}^{k} e_l^{\,2}(j), l = 1,2,3 \quad (14)$$

- Update the lengths:

$$M_1(k+1) = \begin{cases} M_1(k)+1, & if \quad m_1 > m_2 > m_3 \\ M_1(k), & if \quad \begin{cases} m_1 > m_2 \\ m_{22} \le m_{33} \end{cases} \\ M_1(k)-1, & otherwise \end{cases} \quad (15)$$

$$M_2(k+1) = M_1(k+1)+1, M_3(k+1) = M_1(k+1)+2 \quad (16)$$

- Update the step-sizes:

$$\mu_l(k+1) = \frac{\mu N_0}{N_l(K+1)}, l = 1,2,3 \quad (17)$$

$m_i (i = 1,2,3)$ acts as the statistic square error in this algorithm. It is shown in Bilcu et al (2002) that for an uncorrelated input signal $r(n)$ which satisfies $E[r(n)r(n-k)] = 0$ for $k \ne 0$, the following is valid:

$$\frac{J_\infty^{(i)}}{J_\infty^{(j)}} = \frac{J_{\min}^{(i)}}{J_{\min}^{(j)}} = \begin{cases} \ge 1, & if \quad M_1 \le M_2 < M_{opt} \\ < 1, & if \quad M_2 < M_1 < M_{opt} \\ 1, & if \quad M_1 > M or M_2 > M \end{cases}, i = 1,2,3, \quad j = 1,2,3, \quad i \ne j \quad (18)$$

when the following relation holds at each iteration:

$$\mu_1(k) N_1(k) = \mu_2(k) N_2(k) = \mu_3(k) N_3(k) \quad (19)$$

where $J_\infty^{(i)} = E[e^2(\infty)^{(i)}], i = 1,2,3$ is the steady-state MSE, $J_{\min}^{(i)}, i = 1,2,3$ is the minimum steady-state MSE, and M_i is the filter length of the i^{th} filter and M_{opt} is the optimum filter length. Hence in this new algorithm, Equation (15) guarantees the filter length having an optimum value. The second filter is the filter of interest in the sense that its coefficients vector will be the closest one to the Winner filter.

Selecting an optimum L is very important for the algorithm. On the one hand L should be small enough in order to update $m_i (i = 1,2,3)$ quickly. On the other hand L should be large enough to ensure that $m_i (i = 1,2,3)$ is a sufficient statistic. However, unfortunately there is still no theoretical optimum value for L.

Note that Equation (18) would not be valid if the input signal is correlated. However, for this application it can be assumed that the multipath effects sequence for carrier phase is random, i.e. uncorrelated.

Multipath mitigation on position results

The L1 carrier phase DD data are shown in Figure 6, and the L2 data has the similar characteristics (Figure 9). The lowest satellite introduces the worst multipath effects.

As discussed in the last section, the correlated component between successive days' carrier phase DD can be extracted using the LMS filter or VLLMS filter. There are two different filtering processes: forward filtering and backward filtering. Forward filtering means that GPS results on a given day are used to correct results on the following day while backward filtering has the inverse meaning (Ge et al, 2000). According to Liu (2008), forward filtering is better than backward filtering statistically, and the larger the time differenced between reference and input signals, the less effective the multipath mitigation will be. In this paper only forward filtering is used, and the reference signal and input signal are from two successive days.

Figure 10 and Figure 11 show the carrier phase DD of satellites PRN06 and PRN16 before and after filtering. Again, the reference satellite is PRN18. The carrier phase DD data of the first day (day1) acts as the reference signal while the data of the second day (day2) are the input signal (according to the definition of forward filtering). In these two figures, the filtering length (FL) of the LMS filter, the initial filtering length (IFL) and the statistical length L of the VLLMS filter are all one. Only the worst multipath affected parts of the two satellites are shown. From the statistical results in Table 1 and Table 2, the improvement in standard deviation of the carrier phase DD is up to 56.1%, and obviously the VLLMS performs better than the LMS filter.

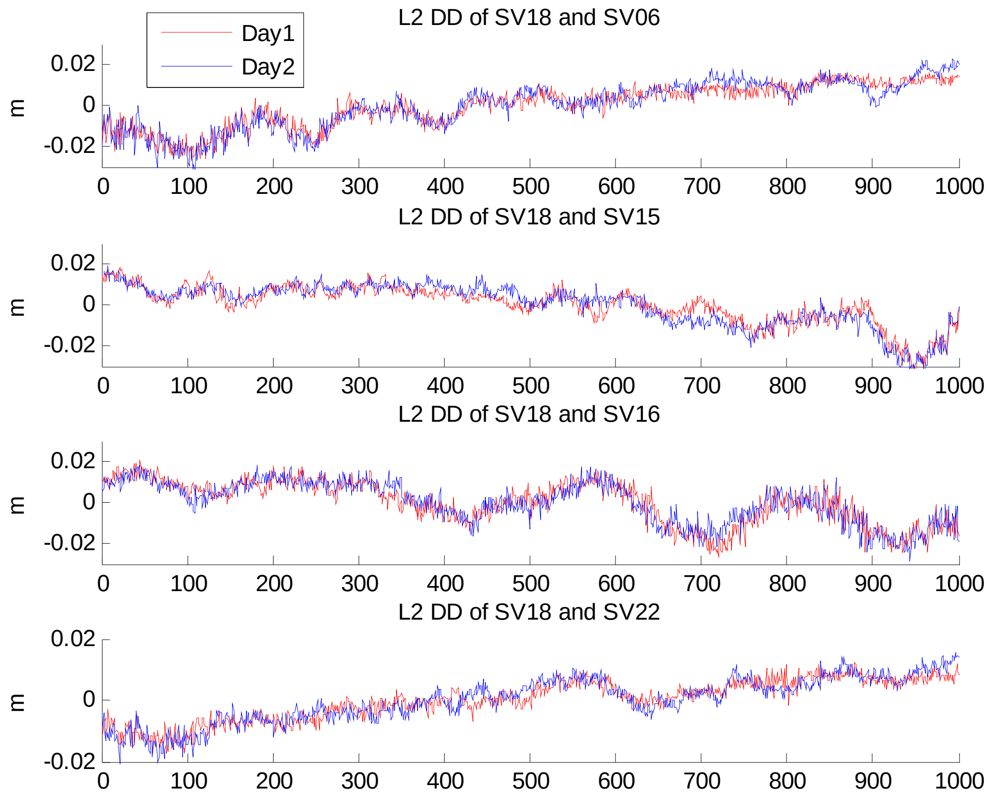

Figure 9: L2 Carrier phase DD data involving Rover and Base receivers.

Table 1: Standard deviation of carrier phase DD of PRN06 (m)

PRN06		Before multipath mitigation	After multipath mitigation	Improvement
L1	LMS filtering	0.00570	0.00382	33.0%
	VLLMS filtering		0.00257	54.9%
L2	LMS filtering	0.00702	0.00531	24.4%
	VLLMS filtering		0.00350	50.1%

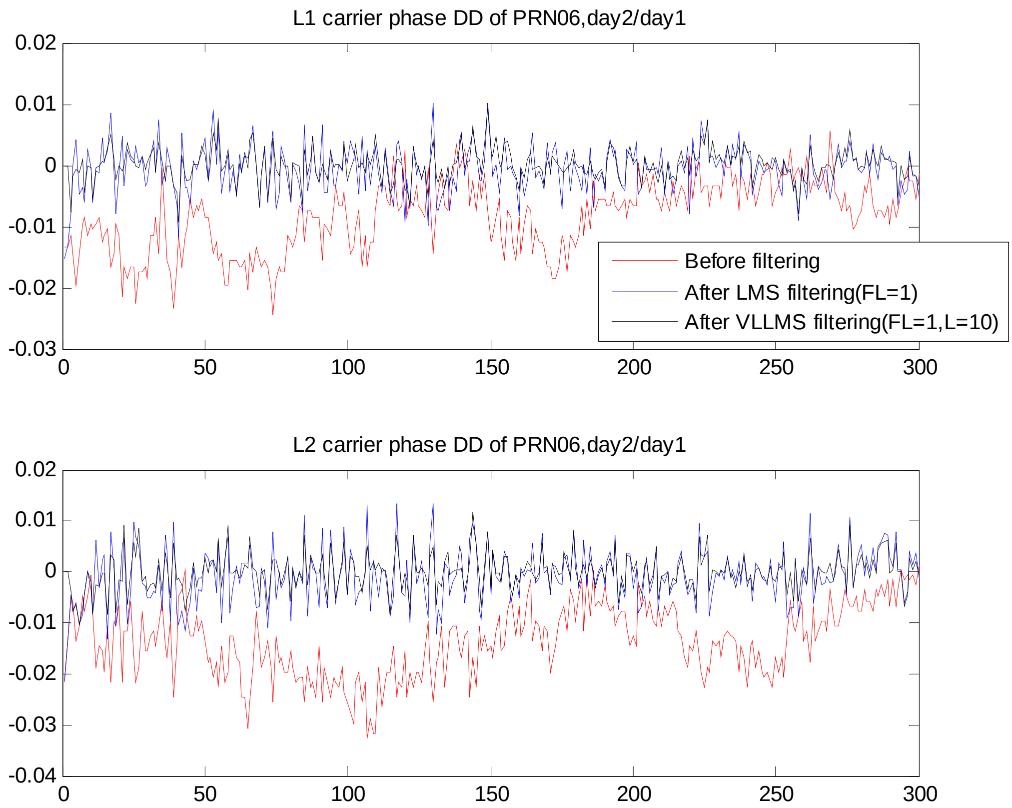

Figure 10: Carrier phase DD of PRN06 before and after filtering.

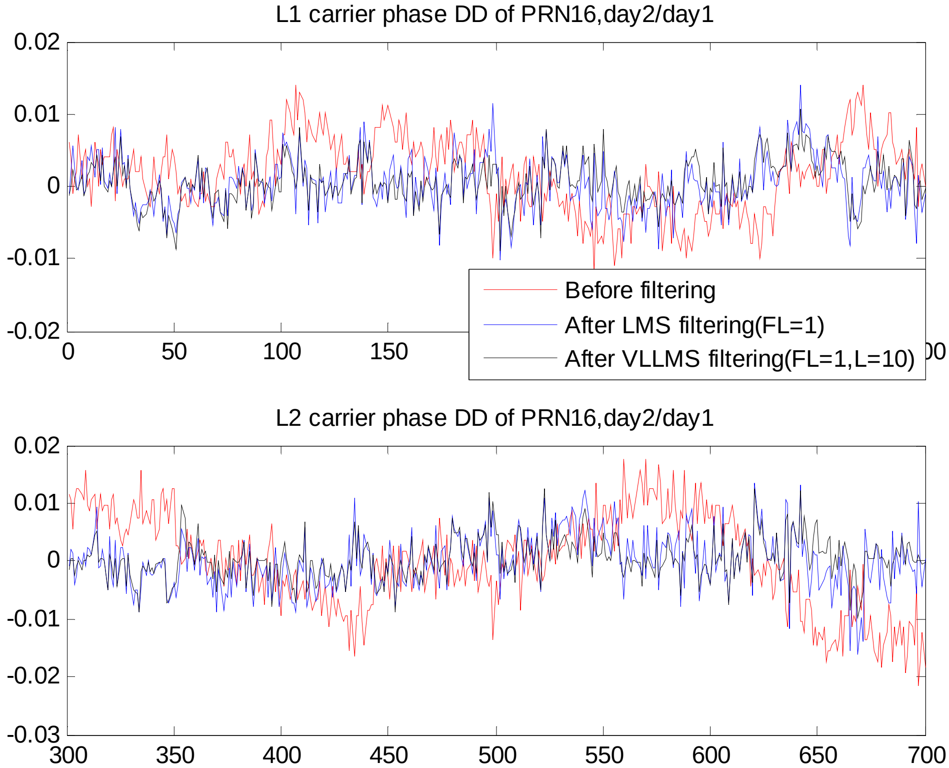

Figure 11: Carrier phase DD of PRN16 before and after filtering.

Table 2: Standard deviation of carrier phase DD of PRN16 (day2/day1)

PRN06		Before multipath mitigation(m)	After multipath mitigation(m)	Improvement
L1	LMS filtering	0.00508	0.00369	27.4%
	VLLMS filtering		0.00306	39.8%
L2	LMS filtering	0.00811	0.00476	41.3%
	VLLMS filtering		0.00356	56.1%

The performance of the two classes of filters can also be analysed in the frequency domain. The correlation characteristics of multipath effects on day1 and day2 can be more clearly seen from their correlation vector's FFT. From Figure 12, where the input signal $r(n)$ is the DD sequence from day1 and the reference signal $d(n)$ represents the DD sequence from day2, it can be concluded that $r(n)$ and $d(n)$ are strongly correlated since the FFT of R_{rd} is not "white", where:

$$R_{rd}(k) = E[r(n)d(n-k)], n,k = 1,...,N. \quad (20)$$

Figure 12 also shows the FFT of R_{ed} for the two filters, where:

$$R_{ed}(k) = E[e(n)d(n-k)], n,k = 1,2...,N. \quad (21)$$

$e(n)$ is the filter's estimation error, which should be uncorrelated with $d(n)$. According to the experiment results shown in Figure 12, the frequency components of R_{rd} are mainly concentrated in the spectrum range 0~0.01Hz. However, after filtering, the FFT of R_{ed} is obviously smoother, which is to say $e(n)$ is more like white noise. Also, $e(n)$ of the VLLMS filter is "whiter" than the $e(n)$ of the LMS filter. As shown by Equation (7), the correlated components between $d(n)$ and $r(n)$ are the multipath effects.

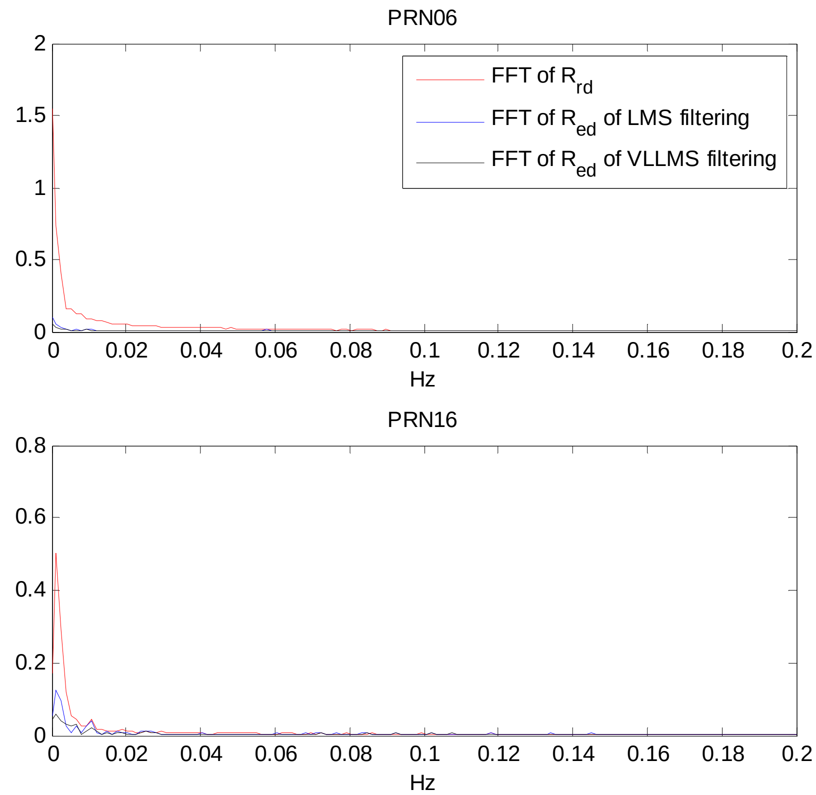

Figure 12: The correlation vector's FFT between input/output signal and reference signal before and after filtering.

Because the elevation of satellite PRN18 is much higher than satellite PRN06 and PRN16, the extracted multipath effects from the two set of DD data can be considered to be the multipath effects on the carrier phase data of satellite PRN 06 and PRN16. Also the assumption can be applied to the other two satellites: PRN15 and PRN22. Then after cancelling the multipath effects from the carrier phase of the four lower elevation satellites, the more accurate position results based on the multipath-mitigated carrier phase data are shown in Figure 13-Figure **15**. Standard deviations of the three coordinate components and the 3-D results are shown in Table 3. From these figures and statistical results, fluctuations that existed before multipath mitigation have been depressed, especially those in the z-coordinate component. The improvement using the VLLMS filter is greater than using the LMS filter,except for the y-coordinate component where the LMS filter performs marginally better (1.5%) than the VLLMS. About 26.3% of the multipath effects on the 3-D positioning can be reduced by using the VLLMS filter, while in the case of the LMS filter, this reduction is about 19.4%.

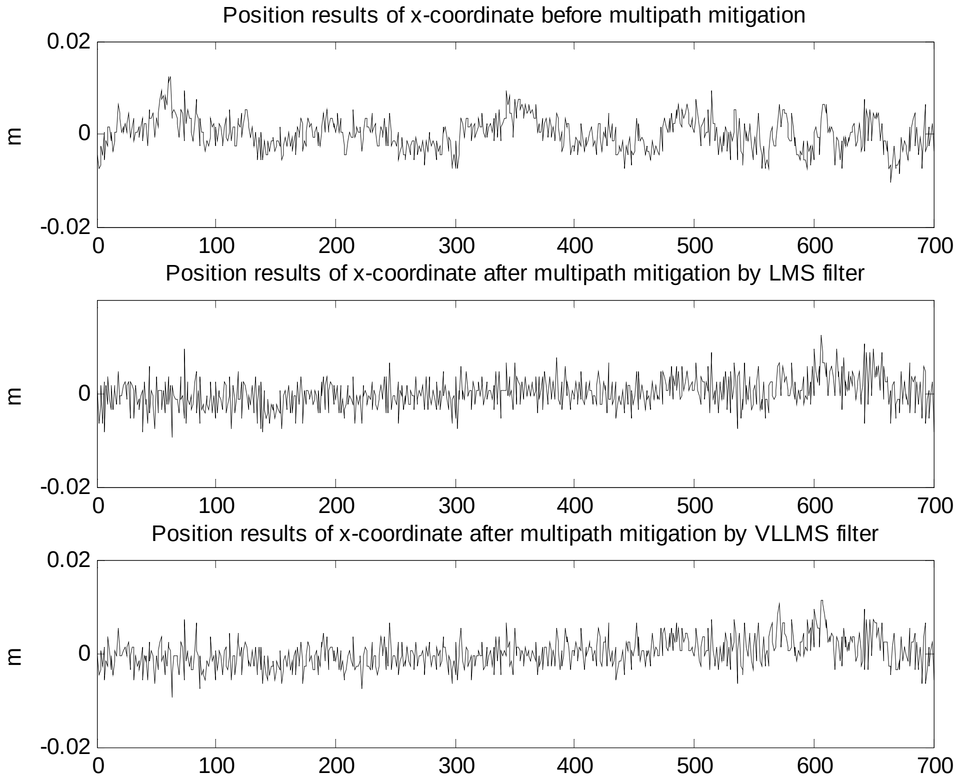

Figure 13: Position results of x-coordinate component from forward filtering (day2/day1).

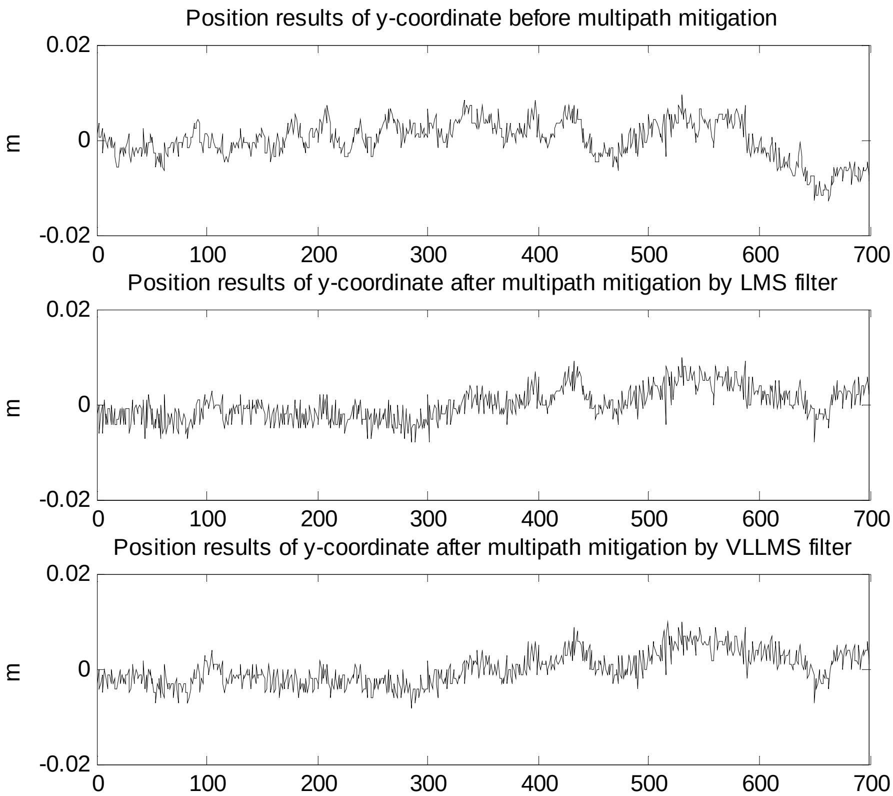

Figure 14: Position results of y-coordinate component from forward filtering (day2/day1).

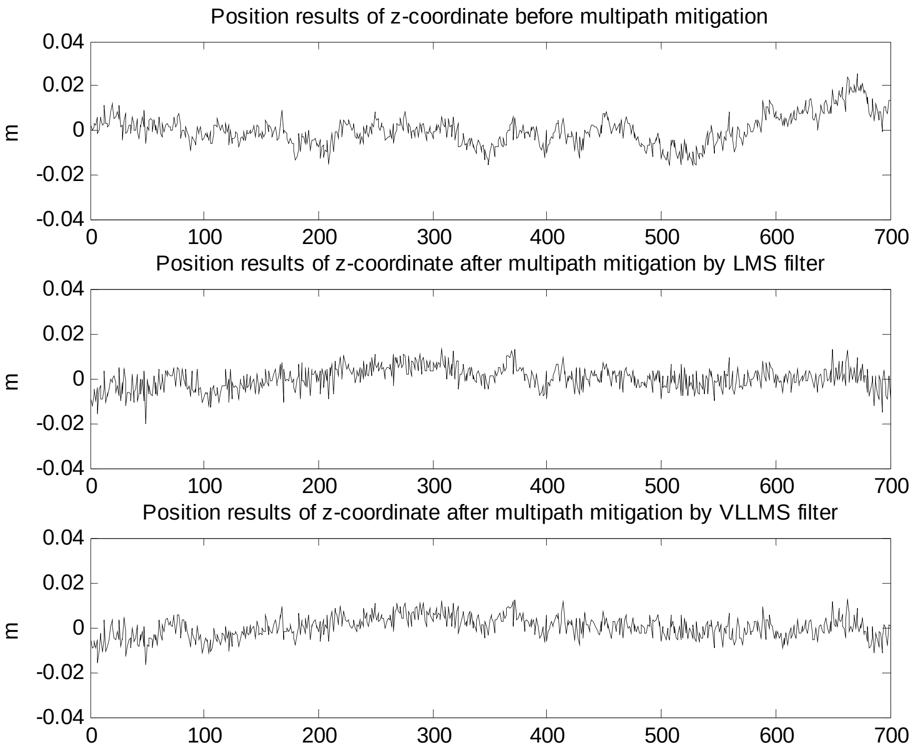

Figure 15: Position results of z-coordinate component from forward filtering (day2/day1).

Table 3: Standard deviation of positioning results (day2/day1)

Standard deviation		Before multipath mitigation(m)	After multipath mitigation(m)	Improvement
X	LMS filtering	0.00359	0.00334	6.96%
	VLLMS filtering		0.00319	11.1%
Y	LMS filtering	0.00400	0.00342	14.5%
	VLLMS filtering		0.00348	13%
Z	LMS filtering	0.00686	0.00495	27.8%
	VLLMS filtering		0.00477	30.5%
3-D	LMS filtering	0.00540	0.00435	19.4%
	VLLMS		0.00398	26.3%

	filtering			

Concluding remarks

In this paper the authors have introduced a multipath mitigation technique based on the VLLMS adaptive filter, and compared its performance with the LMS adaptive filter. Both two filters can extract the multipath effects in carrier phase measurements.

There are three steps to applying the technique. The first step is deriving multipath-effects-dominated DD sequences. A short baseline scenario is necessary. The rover antenna should be set up in a multipath-affected area, while the base antenna should be located in a multipath-free area. During the experiment, a high elevation satellite is observed and serves as the reference satellite so that the multipath effects in the DD data can be considered as the multipath effects of measurements involving the non-reference satellite and the rover antenna. The second step is filtering the DD sequences using the adaptive filter to generate the multipath effects on carrier phase. The third step is removing the multipath effects from the one-way carrier phase measurements and generating more accurate position results.

Experiment results show that the VLLMS filter performs better than the LMS filter, and up to about 26.3% of the multipath effects on the 3-D positioning can be reduced using the VLLMS filter.

References

Fillippov V., Tatarnicov D., Ashjaee J., Astakhov A. and Sutiagin I., The first dual-depth dual-frequency choke ring, The 11th International Technical Meeting of Satellite Division of U.S. ION, September 15-18, 1998, 1035-1040.

Ge L., Han S.W. and Rizos C., Multipath mitigation of continuous GPS measurements using an adaptive filter, *GPS Solutions*, 4:2 (2000), 19-30.

Kaplan E.D. and Hegarty C.J., Understanding GPS: Principles and Applications, second edition, Artech House, 2006.

Liu H., Li X., Ge L., Rizos C. and Wang F, Multipath evaluation of the SydNET CORS receivers based on pseudorange measurements, Journal of Applied Geodesy, accepted.

SydNET page in UNSW website, http://www.gmat.unsw.edu.au/sydnet (accessed July

2008).
Townsend B. and Fenton P., A practical approach to the reduction of pseudorange multipath errors in a L1 GPS receiver. The 7th International Meeting of Satellite Division of U.S. ION, Salt Lake City, September 20-20, 1994, 143-148.
Townsend B., Wiebe I. and Jakab A., Results and analysis of using the MEDLL receiver as a multipath meter, The National Technical Meeting of the U.S. Institute of Navigation, Anaheim, CA, January 2000, 26-29.
Tranquilla J.M., Carr J.P. and Al-Rizzo H.M., Analysis of a choke ring groundplane for multipath control in global positioning system applications, IEEE Transactions on Antennas and Propagation , 42:7 (1994), 905-911.
Van Nee R.D.J., The multipath estimating delay lock loop, The Second Internal Symposium of IEEE on Spread Spectrum Techniques and Applications (ISSSTA'92), Yokohama, Japan, November 29-December 2, 1992, 39-42.
Van Nee R.D.J., Siereveld J., Fenton P. and Townsend B., The multipath estimating delay lock loop: approaching theoretical accuracy limits, IEEE Position, Location and Navigation Symposium, Las Vegas, USA, April 11-15, 1994, 246-251.
Walsh D., Real time ambiguity resolution while on the move, 5th International Technical Meeting of the Satellite Division of the U.S. Institute of Navigation, Albuquerque, NM, September 16 - 18, 1992,473 – 481.